 CMES, vol.4, no.3&4, pp.497-506, 2003

An Anisotropic Damage Model for the Evaluation of Load Carrying Capacity of Composite Artificial Ligaments

P. Vena[1], **R. Contro**

Abstract: The adoption of artificial ligaments in current surgery is still characterised by a low success rate due to the fact that mechanical properties of the biomedical devices are such that a biomechanical compatibility is not fully satisfied. A durable artificial ligament should exhibit stiffness as well as strength properties which are such that a full articulation functionality is guaranteed. To this purpose, reliable numerical methods able to predict the mechanical behaviour of such devices both in the elastic and in inelastic range until complete rupture, could be used for designing of devices with tailored mechanical properties.

The present paper deals with the mechanical characterisation of artificial ligaments made of composite materials, with specific reference to the tensile load carrying capacity. The artificial ligaments taken into consideration are composite cylinders which are manufactured by reinforcing a compliant matrix by means of helicoidally oriented fibres. A finite strain model has been developed and characterised by a stiffness degradation of the reinforcing fibres playing the prominent mechanical role. A suitable choice of the constitutive parameters allowed to reproduce the elastic behaviour and to catch the limit load experimentally measured.

1 Introduction

Substitution of damaged or broken ligaments due to pathologies or injuries is a rather common surgery procedure which can be performed by making recourse to autograft tissues or artificial prostheses. In the first case a tissue sample is harvested from other sites of the patient and implanted in the damaged articulation. In the case of surgery on knee ligaments, the most commonly adopted autograft tissue is part of the patellar tendon which can be easily implanted as a new cruciate ligament. This surgical procedure implies a long post surgery rehabilitation period during which the newly implanted tissue must grow until it gets sufficiently thick and stiff while it is gradually subjected to the physiological loads.

The drawback of the length of the rehabilitation period can be avoided if artificial ligaments are implanted. Artificial ligaments can be subjected to the physiological loads early in the post operative period and the patient can, in principle, restart soon with the normal daily life. Artificial ligaments do not have self-adaptive properties as living tissues do; therefore they have to be previously designed in such a way that all the physiological loads have to be withstood without any unrecoverable damage. Moreover the mechanical response of the biomedical device must be such that the articulation functionality is preserved.

A full functionality can, in principle, be recovered if the mechanical response of artificial ligaments exhibits features similar to those exhibited by natural tissues. The most important mechanical properties of ligaments, that can be assessed by means of laboratory tests, are: the force-displacement curve of a tensile test, the time dependent properties measured by means of creep tests or relaxation tests and the maximum load (load carrying capacity) which can be measured by means of a tensile failure test.

This paper focuses on this latter aspect and aims to present a mathematical model for the determination of the load carrying capacity of artificial ligaments.

The biomedical devices considered in this paper are composite ligaments obtained by means of a double helicoidal Poly-L-Lactide (PLLA) fibre arrangement bonded together by means of a polyethylene matrix. This fibre arrangement is obtained by means of winding machines which allow to control the fibre content and the winding angle. Mechanical laboratory tests have shown that the mechanical behaviour exhibited by such devices, in

[1] Laboratory of Biological Structure Mechanics
Department of Structural Engineering
Politecnico di Milano
Piazza Leonardo da Vinci, 32 – 20133 Milano – Italy

terms of force-displacement curve, is qualitatively similar to that of natural ligaments [Iannace, Sabatini, Ambrosio and Nicolais (1995)]. The main mechanical role is played by the reinforcing fibres which, during longitudinal stretching, exhibit the typical J shaped curve (stiffening effect). This mechanical feature is typical for ligaments and it is a property which is common to most of the living tissues subjected to large strains [Fung (1981)].

The amount of the reinforcing fibres, the winding angle, and their mechanical characteristics should be tuned in order to achieve the full biomechanical compatibility required by articulation functionality.

In this paper the artificial ligament carrying capacity is studied. To this purpose, a continuum damage model suited for anisotropic composite materials is introduced. The model is conceived in the framework of the standard formulation of constitutive equations for dissipative materials consistent with the thermodynamical restriction imposed by Clausius-Duhem inequality. The model is based on the assumption that each constituent (fibre and matrix) can undergo a damage process according to the current state of strain. In particular the numerical examples are carried out under the simplifying assumption that the damage process involves the fibres only. The damage process develops on the basis of the fibre stretch.

The model is formulated within the framework of the finite elasticity theory fulfilling the objectivity principle (material frame indifference [Malvern (1969)]). The formulation allows for the anisotropy of the material, considered as a whole, and for the damage evolution which is related to the anisotropic directions.

Elastic anisotropic material models in finite deformations are widely published in literature with specific reference to biological tissues. More recently, Holzapfel and Gasser (2001) presented a comprehensive paper where both theoretical and computational aspects of viscoelastic anisotropic material models are explored.

Model based on the elastic degradation and progressive damage evolution are present in the literature since the 80's [Krajcinovic (1980, 1996), Murakami (1988)]. These models were formulated for quasi-brittle material such as rocks, ceramics, concrete, etc. More recently anisotropic elastic degradation models have been presented which account for anisotropy induced by a direction dependent damage diffusion, according to the load conditions [Carol, Rizzi and Willam (2001)]. All these models were suited for the small strain kinematic description. However only few works consider the finite strain range. Recently, in [Steinmann and Carol (1998)] one possible extension to the finite strain range has been presented.

More recently other damage models suited for brittle materials based on the evolution of microcracks within the solid have been presented by Chen Z., Hu W. and Chen E.P. (2000).

In the specific field of biological soft tissues few damage models have been published. A finite strain formulation for anisotropic damage diffusion in arterial wall has been presented by Hokanson and Yazdani (1997). This work describes the damage diffusion within an initially isotropic hyperelastic material.

The work presented in this paper deals with initially anisotropic fibrous material, subjected to finite strains under the hypothesis that fibres can undergo stiffness degradation. This assumption is consistent with the experimental and numerical evidence which have shown that the mechanical contribution of the fibres to the load carrying capacity is predominant with respect to that given by the surrounding matrix. When fibres reach a limit threshold, which is a scalar function of the fibre stretch, a degradation of fibre stiffness starts. Damage evolution is governed by a consistency condition similar to that usually defined in the elasto-plastic constitutive modelling. When the fibre has lost its stiffness, the material, which is constituted by the matrix only (exhibiting poor mechanical properties) becomes isotropic.

The model is used for a comparison between the theoretical value of the maximum load and the value estimated during mechanical laboratory tests.

Once the model have proven its effectiveness it can in principle be adopted for tailoring implants with adequate mechanical properties in terms of maximum allowable load. In the last section a brief sensitivity analysis of the load carrying capacity with respect to the main mechanical or geometrical parameters will be presented.

2 Theoretical Model

The constitutive formulation for the composite material adopted in artificial ligament manufacturing is presented in this section. The constitutive theory is cast into the framework of hyperelastic material formulations. The two constituents are characterised by a strain energy function defined in the strain space. These functions are dependent on invariant kinematic quantities. For the specific case of the damage model, the energy associated with the fibres is affected by a damage parameter "D" as follows:

$$W(I_1, I_2, I_3, I_4, D) = W_m(I_1, I_2, I_3) + W_f(I_4, D) \quad (1)$$

where the classical strain invariants are here reported:

$$I_1 = tr(\mathbf{C}) \quad (2a)$$
$$I_2 = \frac{1}{2}\left[(tr\mathbf{C})^2 - tr\mathbf{C}^2\right] \quad (2b)$$
$$I_3 = \det\mathbf{C} \quad (2c)$$
$$I_4 = \mathbf{N}^T\mathbf{C}\mathbf{N} = \lambda^2 \quad (2d)$$

In the previous formulas **C** is the right Cauchy-Green deformation tensor and I_1, I_2, I_3 are the first three strain invariants of the **C** tensor. The fourth invariant I_4 is dependent on the fibre orientation in its undeformed configuration **N** and it is equal to the square of the fibre stretch λ.

In this specific application, the matrix has been assumed to be an isotropic hyperelastic material characterised by the elastic energy W_m and the fibre is characterised by its elastic energy W_f. In particular, the following function has been adopted for the fibre elastic energy :

$$W_f = K_f(1 - D)(I_4 - 1)^4 \quad (3)$$

whereas the strain energy function adopted for the matrix is a slight modification of a formulation introduced by Ogden (1984):

$$W_m = \alpha(I_1 - 3 - \log I_3) + \beta(I_3 - 1)^2. \quad (4)$$

In the formulae (3) and (4) α, β are constitutive parameters related to the matrix and K_f is a constitutive parameter related to the fibres.

The expression for the second Piola-Kirchhoff stress tensor is derived by differentiating the strain energy functions as follows:

$$\mathbf{S} = 2\frac{\partial W(\mathbf{C}, D)}{\partial \mathbf{C}} = \mathbf{S}_m + \mathbf{S}_f = 2\frac{\partial W_m(\mathbf{C})}{\partial \mathbf{C}} + 2\frac{\partial W_f(\mathbf{C}, D)}{\partial \mathbf{C}}. \quad (5)$$

In particular, the stress contribution given by the fibres can be expressed as follows:

$$\mathbf{S}_f = 2\frac{\partial W_f}{\partial I_4}\mathbf{N}\otimes\mathbf{N};$$
$$\mathbf{S}_{f_{ij}} = 2\frac{\partial W_f}{\partial I_4}N_iN_j = TN_iN_j \quad (6)$$

where T is a measure of the fibre tension which, according to equation (3), is:

$$T = 8K_f(1 - D)(I_4 - 1)^3 \quad (7)$$

The damage parameter D has here the meaning of the classic elastic degradation of stiffness. In fact the fibre stiffness parameter K_f can be considered as affected by a coefficient (1-D) which is responsible of the fibre stiffness decay. Fibre stiffness is K_f at the beginning of the strain history when the damage parameter is D=0 and tends to zero as D tends to its maximum allowable value D=1.

The energy put into the unit volume of material in the infinitesimal time interval is given by the tensor product $\mathbf{S}\dot{\mathbf{E}}$, whereas the internal energy variation occurring during the same time interval is $\dot{W}$, which can be expressed as:

$$\dot{W} = \frac{\partial W}{\partial \mathbf{E}}\dot{\mathbf{E}} + \frac{\partial W}{\partial D}\dot{D} = \frac{\partial W}{\partial \mathbf{E}}\dot{\mathbf{E}} - \Delta\dot{D}; \;\; \Delta = -\frac{\partial W}{\partial D} \quad (8)$$

where the symbol Δ can be denoted as damage stress [Manzel and Steinmann (1999)].

The dissipated energy (d) is given by the difference between the energy put in the material and the energy stored within the material as elastic energy. This dissipation "d" must be greater or equal to zero (second principle of thermodynamic) and therefore it must be:

$$\mathbf{S}\dot{\mathbf{E}} - \dot{W} = d \geq 0. \quad (9)$$

If the stresses are defined as in formula (5) the condition on the dissipation reduces to the following simple expression:

$$\Delta\dot{D} \geq 0 \quad (10)$$

and in the case of the specific form of the elastic energy assumed for the fibre it reads:

$$K_f(I_4 - 1)^4\dot{D} \geq 0 \quad (11)$$

For $K_f > 0$ the second principle of thermodynamic reduces to the condition that the damage variable D must be a monotonically increasing parameter, i.e. $\dot{D} \geq 0$.

2.1 Damage criterion

Following the standard scheme of dissipative materials, a limit surface is defined. It delimits the range of elastic behaviour of the material. In the case of damage involving the fibres only, this surface can be reduced to a function depending on a single scalar. In this model a function of the fourth kinematic invariant has been chosen, therefore the general expression of the limit function is as follows:

$$\Psi = \Psi(I_4, D)\,. \tag{12}$$

The elastic behaviour is characterised by the condition $\Psi \leq 0$.

If this condition is met the damage variable does not grow; otherwise the damage increases until the strain state is again within the elastic limit. The damage evolution law is therefore as follows:

$$\begin{cases} \Psi \leq 0 \\ \dot{\Psi} = 0 \end{cases} \Rightarrow \dot{D} = 0; \quad \begin{cases} \Psi = 0 \\ \dot{\Psi} < 0 \end{cases} \Rightarrow \dot{D} = 0\,; \quad \begin{cases} \Psi = 0 \\ \dot{\Psi} > 0 \end{cases} \Rightarrow \dot{D} > 0\,. \tag{13}$$

The evaluation of $\dot{D}$ is given by the consistency condition $\dot{\Psi} = 0$ which assures that the final representative point, in the space of the kinematic variables, will still lie on the limit surface. This condition is quite similar to the consistency condition commonly assumed when elasto-plastic constitutive laws are formulated.

In this work the function Ψ has been chosen as follows:

$$\Psi = \Delta(I_4) - Y_0 - Y(D) \tag{14}$$

where $Y(D)$ is a monotonic increasing function of the damage variable defined in the domain $0 < \mathrm{D} < 1$. In figure 1, two possible shapes of the hardening function Y(D) are reported.

The consistency condition gives the damage rate as follows:

$$\dot{\Delta} + \Psi_Y Y_D \dot{D} = 0$$
$$\dot{D} = -\frac{\dot{\Delta}}{\Psi_Y Y_D} \tag{15}$$

where the index Y or D denotes partial derivative with respect to Y or D respectively.

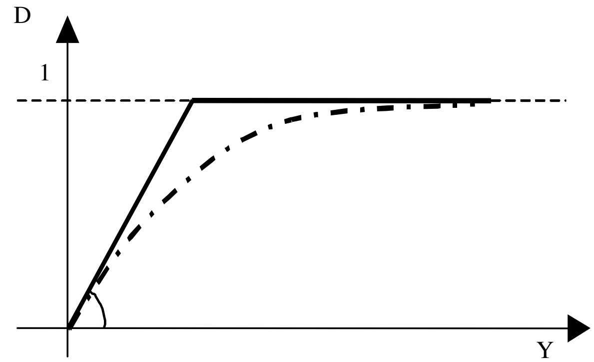

Figure 1 : Two different functions Y(D). The one reported with solid line is that used in the numerical simulations.

In the numerical examples reported in the next section the function Y(D) is assumed as a linear function of the form: $Y = Y_1 D$ and the damage rate is therefore:

$$\dot{D} = \frac{\dot{\Delta}}{Y_1}. \tag{16}$$

The damage rate is given by relation (16) until D reaches its maximum value D=1; thereafter, the damage rate is zero.

In this specific case, simple expressions of the functions $\Delta(I_4)$ and Y(D) have been assumed:

$$\Delta(I_4) = (I_4 - 1)^2 \tag{17a}$$
$$Y(D) = Y_1 D \quad \text{if} \quad D \leq 1 \tag{17b}$$

with this choice the consistency condition can be satisfied exactly by fulfilling the condition $\Psi(I_4, D) = 0$ and consequently:

$$D_n = \frac{\Delta - Y_0}{Y_{01}} \quad \text{if} \quad \dot{D} \neq 0 \tag{18a}$$
$$D_n = D_{n-1} \quad \text{if} \quad \dot{D} = 0 \tag{18b}$$

where the subscript n on the damage variable denotes the value of the variable at the n^{th} computational loading step.

An alternative interpretation of the damaging behaviour can be introduced if the damage phenomenon is described as process responsible for the onset of degrading strains.

The constitutive equation of a damaging fibre can be rewritten in a rate form by differentiating equation (7) as follows:

$$\dot{\mathbf{S}}_f = 8K_f\,(I_4-1)^2\left[3\,(1-D)\,\dot{I}_4-\dot{D}\,(I_4-1)\right]\mathbf{N}\otimes\mathbf{N} \quad (19)$$

where the increment of strain is given by two different contributions: the former is due to the increment of the total deformation and the latter is given by the increment of the damage variable.

Let us now assume a multiplicative decomposition of the I_4 kinematic variable which is the square value of the total fibre stretch by introducing elastic and degrading components in a finite form and in the rate form as in the following:

$$\begin{aligned} I_4 &= I_4^e I_4^D \\ \dot{I}_4 &= \dot{I}_4^e I_4^D + \dot{I}_4^D I_4^e\,. \end{aligned} \quad (20)$$

When, as in equation (20), an elastic strain increment is defined, then the stress increment can be conceived as an elastic constitutive operator applied to the elastic part of the strain increment. Therefore in the case in which for the fibre elastic behaviour a stiffness parameter $\overline{K}$ (which will be in general dependent on the strain itself and damage parameter) is defined, the fibre stress increment can be written as follows:

$$\dot{\mathbf{S}}_f = \overline{K}\dot{I}_4^e\mathbf{N}\otimes\mathbf{N} = \frac{\overline{K}}{I_4^D}\left(\dot{I}_4 - I_4^e\dot{I}_4^D\right)\mathbf{N}\otimes\mathbf{N} \quad (21)$$

in which the elastic strain increment has been obtained by making use of equation (20).

By comparing the two expressions obtained for the stress rates (19,21) the following relations can be obtained:

$$I_4^D = \frac{1}{1-D}\frac{\overline{K}}{24K_f\,(I_4-1)^2} \quad (22a)$$

$$\dot{I}_4^D = \left(I_4^D\right)^2\frac{\dot{D}}{3I_4^e}\,. \quad (22b)$$

These two relations express the equivalence between the degrading strain and the damage variable both in finite and rate forms. From formulae (22) it can be deduced that as damage gets its maximum value (D=1), the degrading strain gets infinite. As a consequence of multiplicative decomposition introduced in equation (20), an infinite value of inelastic strain entails that the elastic component of I_4 goes to zero and consequently the fibre stress vanishes.

A relationship between fibre stress rate $\dot{T}$ and total strain rate (expressed in terms of $\dot{I}_4$) can be determined if equations (16,17) are accounted for:

$$\begin{aligned} \dot{T} &= K_T\,(I_4,D)\,\dot{I}_4 \\ &= 8K_f\,(I_4-1)^2\left[3\,(1-D)-2\frac{(I_4-1)^2}{Y_1}\right]\dot{I}_4 \end{aligned} \quad (23)$$

where K_T is the tangent stiffness which is function of the current strain state and of the damage variable.

The tangent stiffness matrix of the material, which mutually relates the stress and strain conjugate measures, can be expressed in the following general form:

$$\dot{\mathbf{S}} = \frac{\partial\mathbf{S}}{\partial\mathbf{E}}\dot{\mathbf{E}} = \mathbf{K}\,(\mathbf{E},D)\,\dot{\mathbf{E}} \quad (24a)$$

$$\dot{\mathbf{S}} = \dot{\mathbf{S}}_m + \dot{\mathbf{S}}_f = \left[\mathbf{K}_m\,(\mathbf{E}) + \mathbf{K}_f\,(\mathbf{E},D)\right]\dot{\mathbf{E}} \quad (24b)$$

where the damage variable affects the fibre tangent stiffness. The compatibility between fibre and matrix deformations implies that:

$$\mathbf{N}^{\mathbf{T}}\dot{\mathbf{E}}\,\mathbf{N} = \frac{1}{2}\dot{I}_4 \quad (25)$$

and finally the expression of the tangent stiffness can be derived:

$$K_{ijkl}^m\dot{E}_{kl} = \frac{\partial S_{ij}^m}{\partial E_{kl}}\dot{E}_{kl} = \frac{\partial^2 W_m}{\partial E_{ij}\partial E_{kl}}\dot{E}_{kl} \quad (26a)$$

$$K_{ijkl}^f\dot{E}_{kl} = K_T\,(I_4,D)\,N_iN_jN_kN_l\dot{E}_{kl} \quad (26b)$$

where N_i is the i^{th} component of the unit vector parallel to the initial fibre orientation.

The above expounded constitutive law has been implemented into the commercial finite element code ABAQUS (user-defined element fortran routine). The computer code was implemented for a three dimensional brick element with eight node within the standard displacement formulation. Suited compatibility matrixes, which were dependent on the displacement field, were implemented in the framework of a total Lagrangean approach. The nodal residual force vector equivalent to the internal stress components and to the externally applied

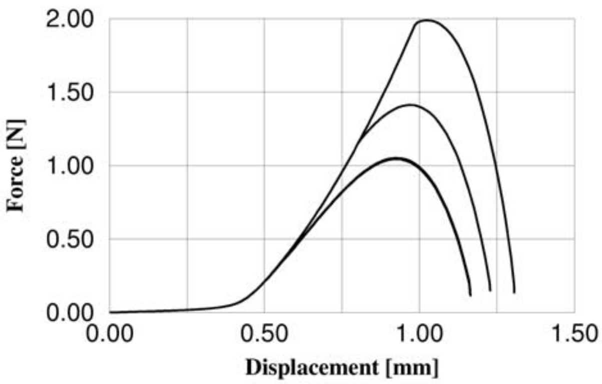

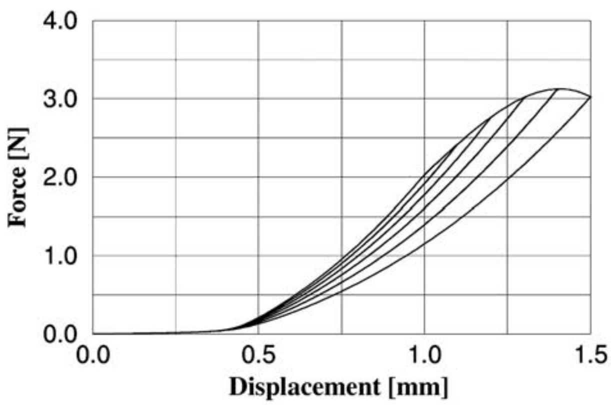

Figure 2 : **(a)** Three tensile tests for different values of the constitutive parameters Y_0. Anisotropy orientation is 45^oin the x-z plane, with z being the stretching direction. **(b)** Cyclic force-displacement curve with increasing maximum stretch.

load, together with the tangent stiffness matrix, were implemented according to Bathe (1982). The contribution given by the anisotropy induced by the fibres was implemented as a simple extension of the standard formulation for isotropic material behaviour.

As an example, uniaxial tensile tests on a unit volume of material are numerically simulated. Let us consider the application of a prescribed stretch along one of the coordinate directions and assume that the anisotropy axes are 45° inclined with respect to the stretching direction. In this case, fibre direction is characterised by the unit vector $\mathbf{N^T} = \left[\begin{array}{ccc} 1/\sqrt{2} & 1/\sqrt{2} & 0 \end{array}\right]$.

As an illustrative example three tensile tests are reported in figure 2a. The three curves are obtained by using the above described model with three different values of the parameter Y_0(0.22, 0.6, 1.3), which accounts for the onset of the degradation of elastic stiffness. The parameter Y_1, which accounts for the growing rate of damage, is kept constant to the value 0.01.

In a further example, a cyclic prescribed displacement with a progressively increasing value of maximum stretch is applied. The stress-stretch behaviour obtained is shown in figure 2b. The material constants where $Y_0 = 1.3$, $Y_1 = 0.1$ Dissipation cycles develop and the stress-stretch curve is such that each reloading path follows the unloading path of previous cycle until new degrading strains develop (or alternatively until new damage develops). The damage rate is zero until the current threshold of the damage limit function is reached. Once the damage reaches its maximum value no stress can be sustained by the fibre at that specific point and the mechanical behaviour of the material is only related to the matrix properties which are not affected by the damage phenomenon.

In these illustrative examples the material parameters characterizing the matrix material were as follows: $\alpha = 0.01$ MPa, $\beta = 1.0$ MPa, whereas the constitutive parameter related to the elastic behaviour of the fibres was assumed to be $K_f = 1.0$ MPa

3 Load carrying capacity of artificial ligaments

One single sample of ligament prosthesis has been subjected to mechanical laboratory tensile tests.

The sample was subjected to a progressively increasing stretch at a constant stretch rate (1/76mm/min) so that a quasi static test is simulated. The tests were stopped when a complete failure was reached.

The artificial ligament subjected to the laboratory tests was a cylinder made of composite material with an average diameter of 4 mm and two helicoidally distributed PLLA reinforcing fibres having a winding angle of 20°. A geometric model of the ligament is reported in figure 3.

The tensile tests carried out within the elastic range allowed to characterise the elastic behaviour and to determine the constitutive parameters presented in the previous section. The values of such parameters are $\alpha = 3$ MPa, $\beta = 5 \cdot 10^{-3}$ MPa, $K_f = 27$ MPa [Figure 4].

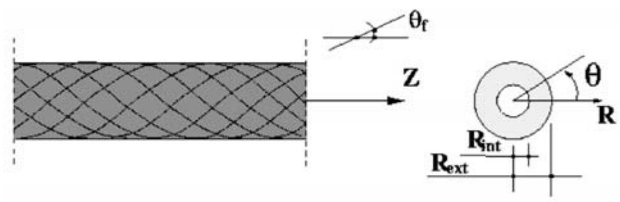

Figure 3 : Geometric model of the artificial ligament: it is a composite tube with reinforcing fibres having a winding angle θ_f.

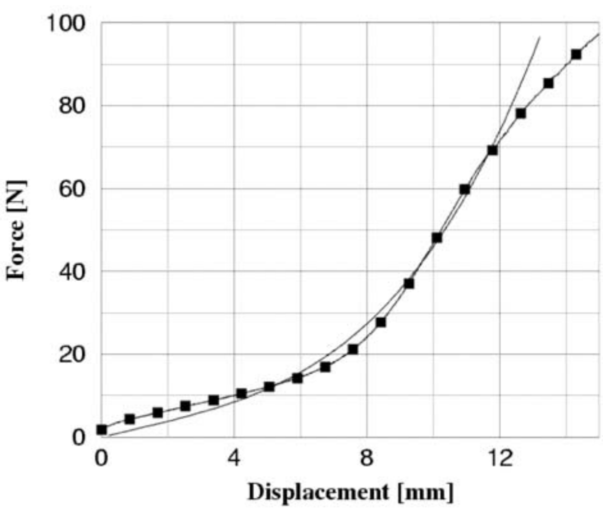

Figure 4 : Comparison between experimental results (line with symbols) and finite element results (solid line) for a tensile test of the artificial ligament within the elastic range.

The initial fibre orientation was such that

$$\overline{N}_1 = -y;\ \overline{N}_2 = -x;\ \overline{N}_3 = \frac{\sqrt{x^2+y^2}}{tg(\theta_f)}$$

$$N_i = \frac{\overline{N}_i}{|\overline{\mathbf{N}}|} \quad (27)$$

where θ_f is the winding angle and (x,y) are the coordinates of the material point in the transversal plane orthogonal to the longitudinal axis.

The elastic behaviour observed from tensile tests is characterised by a typical J shaped force-displacement curve. Such stiffening can be partly ascribed to the non linear behaviour of the constituents and partly ascribed to a kinematic effect, which can be relevant in anisotropic materials. This kinematic effect is given by a progressive variation of the fibre orientation during the strain history and a progressive alignment of fibres along the load direction.

The tensile test carried out up to failure is reported in figure 5. The test showed a maximum load of about 115 N.

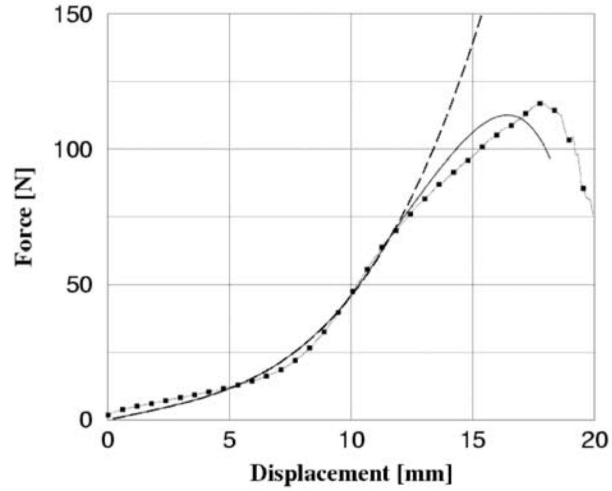

Figure 5 : Comparison between experimental results (line with symbols) and finite element results (solid line) for a tensile test of the artificial ligament until final failure. The purely elastic prediction is also reported as reference (dashed line).

The tensile tests were numerically simulated by using a finite element discretization of the cylinder.

A uniform strain distribution has been assumed along the longitudinal direction and a free transversal deformation was allowed. The finite element model was consisting of 500 hexahedral 8 noded elements with trilinear interpolation of the displacement field.

The longitudinal stretch was simulated by means of uniformly prescribed displacement distribution over the cylinder base.

At increasing load levels, the fibre stretch is not uniform along the radial direction and therefore a non uniform damage distribution is obtained as shown in figure 6a. Higher values of damage are reached at the outer part of the model. The top damage curve provides the damage distribution at the last time step of the load history, when the maximum carrying capacity has already been attained.

The fibre tension T increases until the damage starts to lower the stiffness parameter K_f and, for a given stretch

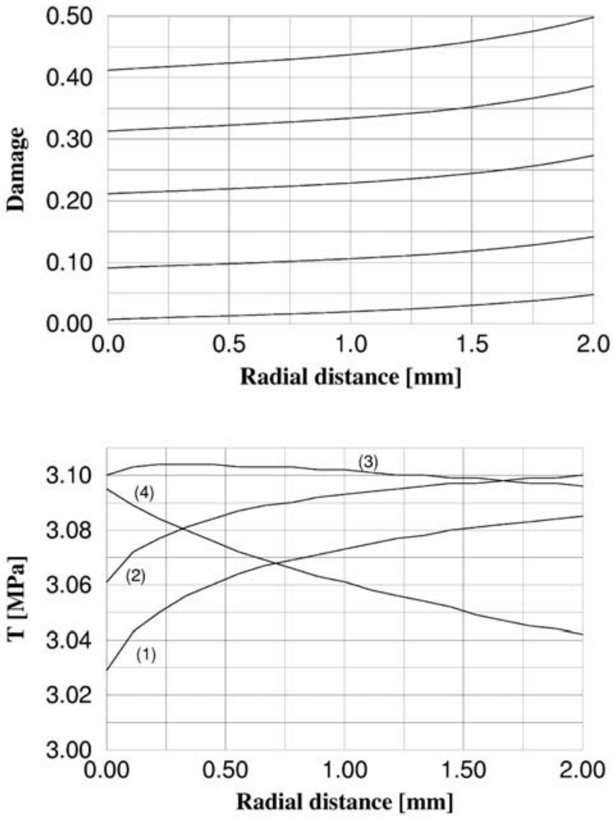

Figure 6 : **(a)** Values of damage variable D within the solid. The distribution of the variable along the radial direction starting from the centre of the model towards the external boundary is reported. Different curves correspond to different load steps. **(b)** Values of variable T (fibre tension) within the solid. The distribution of the variable along the radial direction starting from the centre of the model towards the external boundary is reported. Four analysis steps in the proximity of the maximum load are labelled. The curve (3) corresponds to the fibre tension distribution at the maximum load.

level, T gets its maximum value. In figure 6b , the distribution of fibre tension T along the radial direction within the model is provided at four different time steps.

The curves labelled (1) and (2) refer to two different distributions corresponding to time instants before the load carrying capacity has been reached. When the load reaches its maximum value the fibre tension distribution starts to change its pattern, see curve labelled (3). After the load peak, fibre tension starts to decrease until complete failure is reached, see for example the curve labelled (4).

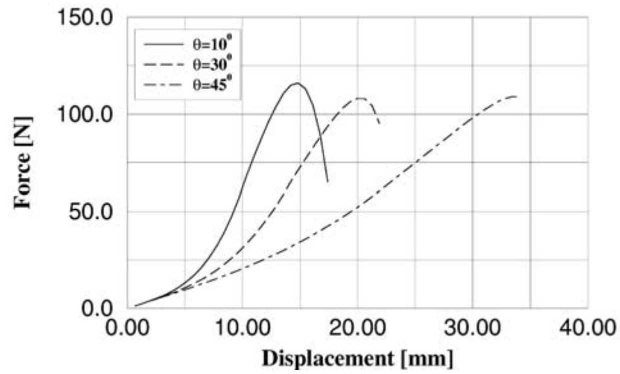

Figure 7 : Force displacement curve predicted by the finite element method for three different winding angles.

A simple trial and error procedure allowed to determine the parameter values of the damage model Y_0 and Y_1. Their values were such that a good agreement between calculated and experimentally evaluated force-displacement curve is obtained. These values resulted Y_0=0.08 and Y_1=0.18.

According to the equations (14) two strain parameters $\bar{\varepsilon}_0$ and $\bar{\varepsilon}_{01}$, which denote the strain levels at which the damage phenomenon starts and complete loss of stiffness is reached, can be defined as follows:

$$\bar{\varepsilon}_0 = \bar{\lambda}_0 - 1 = \sqrt{\sqrt{Y_0}+1} - 1 \quad (28a)$$

$$\bar{\varepsilon}_{01} = \bar{\lambda}_{01} - 1 = \sqrt{\sqrt{Y_0+Y_{01}}+1} - 1 \quad (28b)$$

For the parameters of this simulation one gets $\bar{\varepsilon}_0 = 0.13\,mm/mm$ and $\bar{\varepsilon}_{01} = 0.23\,mm/mm$ which are consistent with the failure strain of the single fibre provided by the manufacturer, which was 0.23 mm/mm.

The model prediction of the tensile behaviour of ligaments with three different winding angles (45^o, 30^o and 10^o) is reported in figure 7.

From the model it comes that the peak load exhibits low sensitivity to the fibre orientation. On the contrary, the rupture strain and the elastic behaviour are much more influenced by this parameter.

4 Conclusions

In this paper an anisotropic damage model that describes the mechanical behaviour of composite artificial ligaments has been presented, with particular emphasis on the evaluation of the load carrying capacity. This is one of the most crucial aspects of the mechanical performance of biomedical devices which have to be taken into account when effective and durable prostheses have to be designed.

The constitutive law is formulated within the framework of the finite hyperelasticity. The loss of load bearing capacity is simulated by means of progressive degradation of elastic parameters. This degradation is provided by a standard damage based model which has been extended to the case of anisotropic and finite strain elasticity. This model does not take into account any fibre-fibre or fibre-matrix interaction. To this purpose a new form of the potential energy with interaction between matrix strain and fibre stretch should be conceived.

The model exhibited good quantitative agreement between experimental and numerical response of the non linear elastic properties and in the evaluation of the maximum load.

Once the model parameters have been identified by comparison between numerical and experimental data of monotonic tension tests, a proper validation would be required. Experimental data of tensile tests conducted on samples manufactured with different fibre winding angles could be useful to this purpose.

The predictive model of the tensile behaviour of ligaments with winding angle of 45°, 30° and 10° provided useful information that can be used for design purposes.

The peak load seems to have low sensitivity to the fibre orientation, whereas, the failure strain and the elastic behaviour is much more influenced by this geometric parameter. These results derived from the fact that the ultimate load is mainly dependent on the fibre strength itself. The contribution of kinematic non linearity is, in this case, not sufficiently effective to suggest the improvement of the ligament strength just by changing fibre arrangements.

The parametric analysis would underline that if the strength of ligaments is of concern, the geometric arrangements of the fibres are of little interest and new fibres with better mechanical properties should be considered. On the contrary, if the elastic behaviour is of more concern, the fibre orientation should be carefully designed in order to tailor a biomedical device which fulfils the clinical requirements. If a rather compliant device and, at the same time, a high failure load is the goal, then a compromise should be found between a proper fibre orientation and the mechanical properties of the single fibres.

Acknowledgement: The financial support for this research was provided by the PFMSTA II project of the National Council of Research (CNR). This support is gratefully acknowledged.

References

Bathe, K.J.; (1982): Finite element procedure in engineering analysis, *Prentice-Hall, New Jersey* .

Carol, I.; Rizzi, E.; Willam K. (2001): On the formulation of anisotropic elastic degradation. I. Theory based on a pseudo-logarithmic damage tensor rate, *International journal of Solid and Structures*, vol. 38, n. 4 pp. 491-518.

Chen, Z.; Hu,W.; Chen, E.,P. (2000): Simulation of dynamic failure evolution in brittle solids without using nonlocal terms in the strain-stress space, *CMES: Computer Modeling in Engineering & Sciences*, vol. 1, n. 4, pp.57-62.

Fung, Y.C. (1981): Biomechanics: mechanical properties of living tissues. *Springer-Verlag, New York.*

Hokanson, J.; Yazdani, S. (1997): A constitutive model of the artery with damage, *Mechanical Research Communications*, vol. 24, n. 2, pp. 151-159.

Holzapfel, G.A.; Gasser, T.C. (2001); A viscoelastic model for fiber-reinforced composites at finite strains: Continuum basis, computational aspects and applications. *Computer Methods in Applied Mechanics and Engineering*, Vol. 190, pp.4379-4403.

Iannace, S.; Sabatini, G.; Ambrosio, L.; Nicolais, L. (1995): Mechanical behaviour of composite artificial tendons and ligaments. *Biomaterials*, pp. 675-679.

Krajcinovic, D.(1996): Damage mechanics. *North-Holland, Amsterdam*.

Krajcinovic, D. (1980): Continuum model of medium with cracks, *ASCE, Journal of Engineering Mechanics*, Vol. 106, pp. 1039-1051.

Malvern, L.E. (1969): Introduction to the mechanics of continuous medium. *Prentice-Hall, New Jersey*.

Manzel, A; Steinmann, P. (1999): A theoretical and computational setting for geometrically non linear damage mechanics, *Proceedings of European Conference on Computational Mechanics, Munich, Germany*.

Murakami, S. (1988): Mechanical modeling of material damage, *Journal of Applied Mechanics*, vol. 55, pp. 280-286.

Ogden, R. W. (1984): Non linear elastic deformations, *Ellis Horwood Series in Mathematics and its applications, Chichester*.

Steinmann, P.; Carol, I. (1998): A framework for geometrically non linear continuum damage mechanics, *International Journal of Engineering Sciences*, vol. 151, pp. 513-538.